iScience

Article

Light intensity-dependent arrestin switching for inactivation of a light-sensitive GPCR, bistable opsin

Graphical abstract

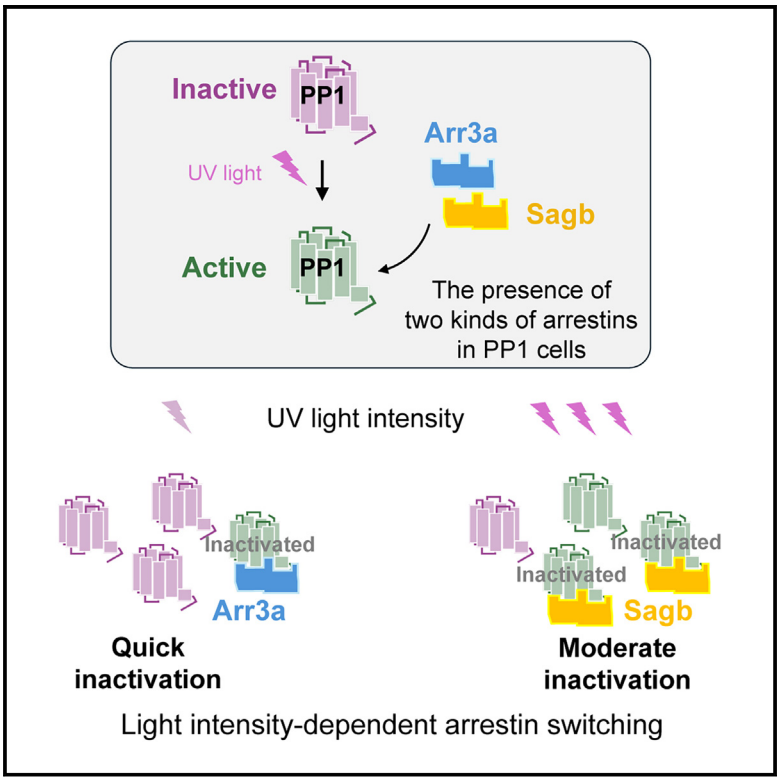

Highlights

- Two kinds of arrestins, Arr3a and Sagb, are expressed in larval zebrafish PP1 cells
- Inactivation of PP1 by Arr3a and Sagb switches depending on light intensity
- Rhodopsin kinase (GRK) is required for PP1 Inactivation by the two arrestins
- The PP1-arrestin complex dissociates by the PP1 back-reaction upon visible light

Authors

Baoguo Shen, Seiji Wada, Tomohiro Sugihara, ..., Takeaki Ozawa, Mitsumasa Koyanagi, Akihisa Terakita

Correspondence

terakita@omu.ac.jp

In brief

Biochemistry; Protein

Shen et al., 2025, iScience *28*, 111706
February 21, 2025
https://doi.org/10.1016/j.isci.2024.111706

CellPress

iScience

CellPress
OPEN ACCESS

Article

Light intensity-dependent arrestin switching for inactivation of a light-sensitive GPCR, bistable opsin

Baoguo Shen,[1,2,5,7] Seiji Wada,[1,2,3,6,7] Tomohiro Sugihara,[1,2] Takashi Nagata,[2] Haruka Nishioka,[2] Emi Kawano-Yamashita,[2] Takeaki Ozawa,[4] Mitsumasa Koyanagi,[1,2,3] and Akihisa Terakita[1,2,3,8,*]

[1]Department of Biology, Graduate School of Science, Osaka Metropolitan University, 3-3-138 Sugimoto, Sumiyoshi-ku, Osaka 558-8585, Japan

[2]Department of Biology and Geosciences, Graduate School of Science, Osaka City University, 3-3-138 Sugimoto, Sumiyoshi-ku, Osaka 558-8585, Japan

[3]The OMU Advanced Research Institute for Natural Science and Technology, Osaka Metropolitan University, 3-3-138 Sugimoto, Sumiyoshi-ku, Osaka 558-8585, Japan

[4]Department of Chemistry, School of Science, The University of Tokyo, 7-3-1 Hongo, Bunkyo-ku, Tokyo 113-0033, Japan

[5]Present address: State Key Laboratory of Ophthalmology, Optometry and Vision Science, Wenzhou Medical University, Wenzhou, Zhejiang 325027, China

[6]Present address: Department of Chemistry and Biological Science, College of Science and Engineering, Aoyama Gakuin University, 5-10-1 Fuchinobe, Chuo-ku, Sagamihara-shi, Kanagawa 252-5258, Japan

[7]These authors contributed equally

[8]Lead contact

*Correspondence: terakita@omu.ac.jp

https://doi.org/10.1016/j.isci.2024.111706

SUMMARY

Inactivation of most light-sensitive G protein-coupled receptor (GPCR) opsins involves arrestin binding to terminate cell responses. In the zebrafish pineal organ, UV sensitive parapinopsin 1 (PP1)-expressing cells exhibit color opponency through photoequilibria between two photo-interconvertible states of PP1. The amount of visible light-sensitive active states (photoproducts) is crucial for generating color opponency, raising questions about how and what arrestins are involved in PP1 inactivation. Here, we found two arrestins, Arr3a and Sagb competitively bind to PP1. Photoresponse analyses of the PP1 cells using gene-knockdown larvae revealed Arr3a-involved quick inactivation was switched to Sagb-involved moderate inactivation depending on increased light intensity. Furthermore, we found photoregeneration of PP1 facilitates the dissociation of the PP1-arrestin complex, allowing for continuous arrestin supply in the photoequilibria under strong light. These regulations for the active photoproduct amounts of PP1 may help maintain appropriate color opponency. The current findings provide insight into the dynamics of GPCR inactivation involving multiple arrestins.

INTRODUCTION

Photoreceptor cells have inactivation mechanisms for quick termination of photoresponses initiated following light absorption by opsins. Previous studies on vertebrate visual cells (i.e., ocular photoreceptor cells for vision) have shown that photoactivated opsin-based pigments, namely rhodopsin and cone pigments, are phosphorylated by opsin kinases and then bound to arrestins to be completely inactivated.[1–11] Gene knockout of opsin kinase or arrestin in rod cells in mice delays termination of the electrophysiological photoresponse, resulting in a prolonged response.[5,10] Many vertebrates have multiple genes encoding rhodopsin kinase and arrestin. Some subtypes are expressed in rods and cones, which are involved in dim light and day light vision, respectively. Of the rhodopsin kinases, GRK1 and GRK7 are the major subtypes contributing to termination of photoresponses in rods and cones and are referred to as rod- and cone-type, respectively. However, expression profiles of GRKs in rods and cones throughout vertebrates are complicated. For example, in humans, GRK1 is expressed in rods and cones whereas GRK7 is expressed only in cones.[6] The mouse genome harbors GRK1, expressed in rods and cones but not GRK7.[12,13] In some species, GRK1 is exclusively expressed in rods.[6] In zebrafish, GRK1a is expressed in rods but GRK1b and 7a are expressed in cones.[14] For arrestins, rods express arrestin1 but cones express both arrestin1 and arrestin4 in mice. In zebrafish, rods express Saga and Sagb, homologs to mouse arrestin1, but cones express Arr3a and 3b, homologs to mouse arrestin4.[15,16]

In many non-mammalian vertebrates, pineal organs, as well as eyes, contain photoreceptor cells,[17–20] some of which express opsins distinct from those expressed in ocular rods and cones.[21–26] We previously revealed that a pineal-specific UV-sensitive opsin named parapinopsin (PP; PP1 in teleost) is expressed in a type of pineal photoreceptor cell that is involved in antagonistic

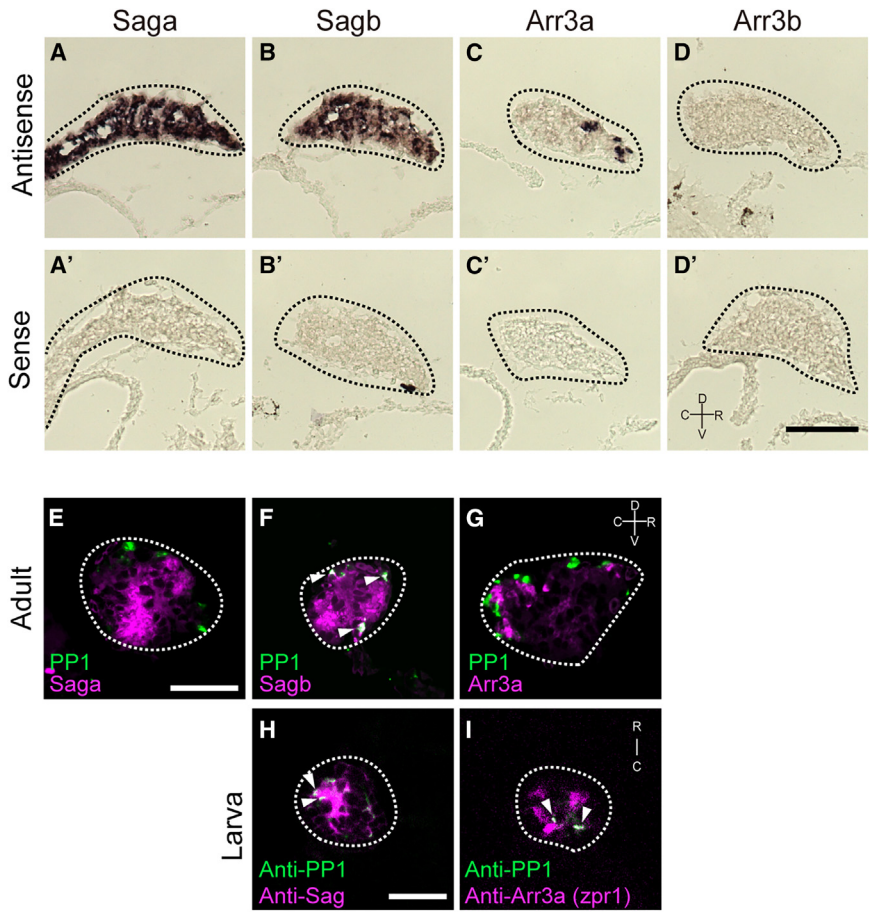

Figure 1. *In situ* hybridization and immunohistochemical analyses of arrestins in the zebrafish pineal organ

(A–D, A′–D′) *In situ* hybridization to evaluate mRNA expression of arrestin subtypes Saga, Sagb, Arr3a, and Arr3b in the pineal organ of adult zebrafish. The orientation is shown using rostral (R), caudal (C), dorsal (D), and ventral (V) sides; scale bar, 50 μm.

(E–G) Double fluorescence *in situ* hybridization analyses of PP1 vs. Saga (E), vs. Sagb (F), and vs. Arr3a (G) in the pineal organ of adult zebrafish; scale bar, 50 μm.

(H and I) Whole-mount immunohistochemical analyses using anti-PP1 and anti-Sag (H), and anti-Arr3a (zpr1, I) antibodies. PP1 cells in 5-dpf larvae express Arr3a and Sag; scale bar, 20 μm. Dotted traces indicate landmarks of the pineal organ (A–I). Arrowheads indicate the co-expression of arrestins and PP1 (F, H, and I).

chromatic responses to UV and visible light.[21,23] PP has a molecular property called "bistable nature," which is different from that of visual opsins such as rhodopsin and cone opsins.[21,23,26,27] Upon UV absorption, the dark state of PP1 converts to a photoproduct, which is the active state activating a G protein, transducin 2 (i.e., the cone-type transducin), in pineal photoreceptor cells.[21] The photoproduct, which has an absorption maximum in the visible light region, is stable and reverts to the original dark (inactive) state upon visible light absorption. Our previous study revealed that a single pineal photoreceptor cell generates color opponency using a single type of opsin, PP1, in the zebrafish pineal organ because of the bistable nature of PP1.[26] Under physiological light conditions, which comprise a broad range of wavelengths, different photoequilibria are formed between the dark state and photoproduct, depending on the spectral distribution of light. The change in spectral components of the UV and visible light region (e.g., the change in spectral components from shady to sunny locations) changes the amount of the photoproduct activating G proteins. Color opponency in the PP1-expressing cell is generated based on a change in the amount of PP1 photoproduct that activates G protein. Thus, dark inactivation of PP1 photoproducts by dark inactivation-related proteins, such as GRK and arrestin, greatly affects the amount of "active" PP1 photoproducts. We previously found that PP1-based color opponency is observed under light conditions that are equivalent to the sunny region in the late afternoon.[26]

We performed simulations varying the time constant for the dark inactivation of active PP1 photoproducts on forming a photoequilibrium under the light conditions described previously. The results suggested that when dark inactivation goes on with too small time constant (too fast reaction rate), an insufficient amount of the active PP1 photoproduct is available to accurately capture color information at the light intensities. Therefore, a dark inactivation system that maintains an appropriate amount of the active PP1 photoproduct may be essential to obtain accurate color information based on PP1 under physiological light conditions. Therefore, both the photoequilibrium of PP1 and the dark inactivation system for PP1 photoproduct are important for generating color opponency based on PP1.

We recently found that zebrafish PP1-expressing photoreceptor cells use rhodopsin kinase GRK7a, which is known to be involved in the inactivation of cone opsins through phosphorylation, to achieve inactivation of PP1.[24] However, what types of arrestin are involved in the inactivation mechanisms in PP1 cells has not been determined. In this article, we attempted to identify arrestins contributing the inactivation of PP1 in zebrafish larvae and found that two visual arrestins, Arr3a and Sagb, inactivate PP1 cooperatively but with different kinetics.

RESULTS

Sagb and Arr3a as candidate molecules involving dark inactivation for PP1

The zebrafish genome harbors seven arrestin genes, three non-visual arrestins (β-arr1, β-arr2a, and β-arr2b) and four visual arrestins (Saga, Sagb, Arr3a, and Arr3b).[16,28,29] To determine what types of arrestins are expressed in the zebrafish pineal organ, we performed *in situ* hybridization and found that Saga, Sagb, and Arr3a are strongly expressed in the pineal organ of

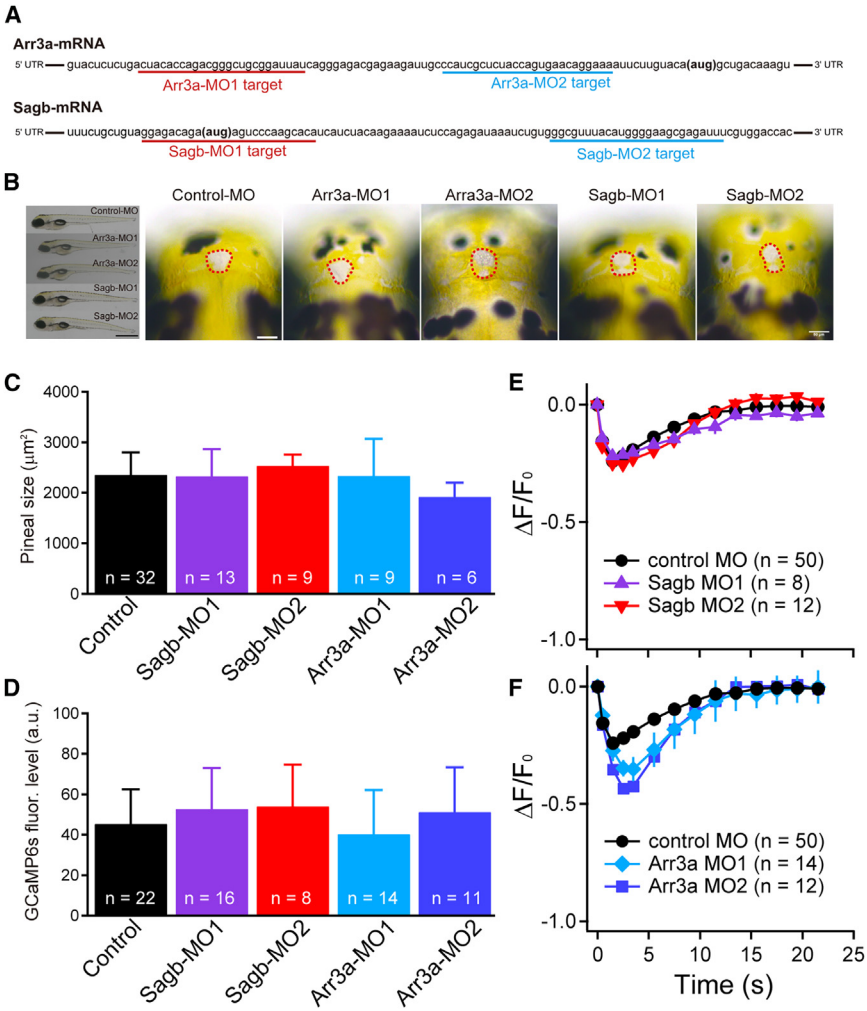

Figure 2. Antisense morpholino oligo (MO)-mediated knockdown of Sagb and Arr3a in zebrafish larvae

(A) Nucleotide sequences of Sagb and Arr3a mRNAs in zebrafish. Red (MO1) and blue (MO2) underlines indicate targeted sequences; "aug" in parentheses in each sequence indicate start codons.

(B) (left) Images showing whole bodies of 5 dpf larvae injected with control-MO, Sagb-MO1, Sagb-MO2, Arr3a-MO1, and Arr3a-MO2; scale bar, 1 mm. (right) Dorsal views of pineal organs of 5 dpf larvae injected with control or each arrestin-MO. Landmarks indicate pineal organs; scale bar, 50 μm.

(C) Quantitative analyses of larval pineal size in B (right). Error bars indicate standard deviation. Significant differences between control and the other morphant fish were not found (*p* values for control vs. all are > 0.05; Dunnett's multiple comparison test).

(D) Quantification of GCaMP6s fluorescence intensity in larvae injected with control-MO and arrestin-MO. Error bars indicate standard deviation. Significant differences between control and the other morphant fish were not found (*p* values for control vs. all are > 0.05, Dunnett's multiple comparison test).

(E and F) Calcium changes upon 405-nm laser flashes showing effects of Sagb and Arr3a knockdown using designed MOs on the light response in PP1 cells. Control (black closed circle), Sagb-MO1 (purple triangle), and Sagb-MO2 (red inverted triangle) injected larvae (5 dpf) exhibited similar responses (n = 50, 8, and 12 in (E), respectively). Arr3a-MO1 (skyblue oblique square) and Arr3a-MO2 (blue square) injected larvae (5 dpf) exhibited similar responses (n = 50, 14, and 12 in (F), respectively) to each other but both exhibited different profiles from control fish.

adult stages (Figures 1A–1D, A′-D′); both Saga and Sagb are more broadly expressed than Arr3a in the pineal organ. The expression of β-arrestins was not clearly observed (Figure S1). Double fluorescence *in situ* hybridization revealed that Sagb was expressed with PP1, which is expressed in a limited number of pineal photoreceptor cells[21] (Figure 1F, arrowheads), indicating that Sagb is one of the candidates involved in the dark inactivation of PP1. In contrast, co-expression of PP1 with Saga or Arr3a was not observed (Figure 1E and G). Further immunohistochemical analysis of arrestin expression in the larval pineal organ revealed Sag expression in larval PP1 cells (Figure 1H, arrowheads). Unexpectedly, we found that Arr3a was also expressed in larval PP1 cells (Figure 1I, arrowheads). Thus, we found these two arrestins as candidates involved in the dark inactivation of PP1 in the larval zebrafish.

Functional dark inactivation of PP1 by switching Sagb and Arr3a depending on light intensity

To verify the relationship between the two arrestins and PP1-evoked photoresponses by gene knockdown, we designed antisense morpholino oligos (MOs) against the two arrestins (Figure 2A). Note that Arr3a MO1 is identical to that previously reported, and therefore its strong knockdown effect has already been confirmed.[16] Morphant fish did not show an abnormal phenotype in whole-body morphology or pineal size compared with controls (Figures 2B and 2C). To capture PP1 photoresponses, MOs were injected into embryos the 1-cell stage from a strain in which GCaMP6s, a fluorescent calcium indicator, is expressed in PP1 cells, *Tg(pp1:GCaMP6s)*.[26] Because vertebrate photoreceptor cells in the pineal organ as well as the retina exhibit intracellular calcium decreases together with the hyperpolarization in a light-dependent manner, calcium imaging is available to record photoresponses in PP1 cells. GCaMP6s expression in morphant PP1 cells was confirmed, and a significant difference in fluorescent levels was not found between control and morphant fish (Figure 2D). To observe the effect of the MOs in PP1 photoresponses, we performed two-photon live imaging of *Tg(pp1:GCaMP6s)* with stimulus using a 405-nm laser. After the fluorescence images of dark-adapted fish were initially obtained (F_0 images), fish were exposed to a 405-nm laser flash (~450 ms). Subsequently, images after an interval (t) were obtained (F_t images). Images obtained after different intervals

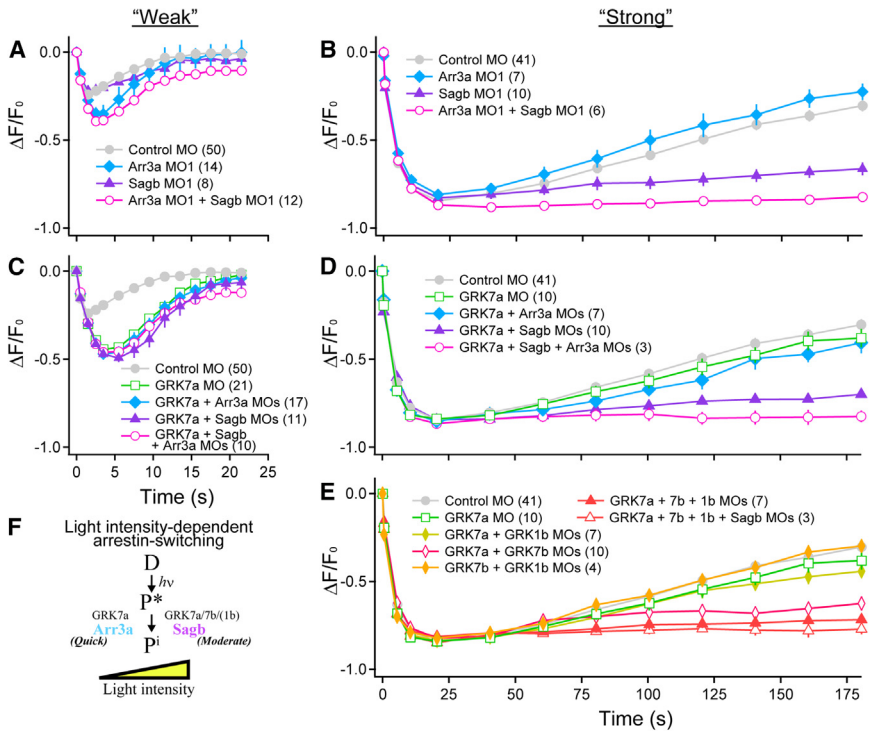

Figure 3. Investigation of rate-determining molecules in the process of response termination in PP1 cells by multiple genes-knockdown

(A and B) Response profiles in control (gray closed circle), Arr3a (skyblue oblique square), Sagb (purple closed triangle), and both Arr3a and Sagb (magenta open circle) MO-injected larvae (5 dpf). Sagb knockdown under Arr3a knockdown background led to a later response termination against "weak" light flash compared with Arr3a single knockdown (A). Arr3a knockdown under Sagb knockdown background led to a later response termination against "strong" light flash compared with Sagb single knockdown (B).

(C and D) Response profiles in Arr3a (skyblue oblique square), Sagb (purple closed triangle), and both Arr3a and Sagb (magenta open circle) MO-injected larvae (5 dpf) under the background of GRK7a knockdown. Against a "weak" light flash, the response termination was similar to that of GRK7a single-knockdown fish (C, green open square), indicating that the rate-determining molecule in the response is GRK7a. In contrast, against a "strong" light flash, GRK7a single-knockdown fish was comparable to control fish (D, green open square, gray closed circle). GRK7a and Arr3a double-knockdown fish (D, skyblue oblique square) exhibited similar response profile to the GRK7a single-knockdown and control fish but differed from the GRK7a and Sagb double-knockdown fish (D, purple closed triangle). Furthermore, GRK7a/Arr3a/Sagb triple-knockdown fish (D, magenta open circle) exhibited the latest response termination.

(E) Response profiles against a "strong" light flash in GRKs-MO (7a/1b in yellow closed diamond, 7b/1b in orange closed diamond, 7a/7b in red open diamond, and 7a/7b/1b in red closed triangle) injected larvae (5 dpf). Sagb knockdown fish under the GRK7a/7b/1b triple-knockdown background (red open triangle) exhibited a similar termination process to the GRK7a/7b/1b triple-knockdown fish (red closed triangle). Error bars indicate standard error. The duration of each stimulus was ~450 ms. The 405-nm laser intensities are ~6.0×10^{14} photons/cm^2/s in (A) and (C) and ~5.0×10^{16} photons/cm^2/s in (B), (D), and (E). Numbers in parentheses indicate the number of individuals. Statistical analysis was performed on amplitudes, slopes, area, and time to peak (see additional file, Figure S3).

(F) Summary of molecules related to PP1 inactivation.

allowed us to draw profiles as a series of responses, eliminating the extra effect of two-photon laser excitation against PP1. In PP1 photoresponse, Sagb knockdown fish with each MO were not largely different from control fish (Figure 2E). In contrast, Arr3a knockdown fish with both MOs showed clearly different response profiles, with larger amplitudes, compared with control fish (Figure 2F) and Sagb knockdown fish (see the statistical analyses in Figure S3). In addition, the response profiles in Arr3a knockdown fish tended to show delayed peaks compared to those in control fish. These observations indicate that the response termination was affected by Arr3a knockdown. Therefore, Arr3a is thought to be one of the major players involved in inactivation of PP1.

In contrast to the knockdown effects of Arr3a MOs on PP1 photoresponses, neither Sagb MO1 nor MO2 exhibited a knockdown effect. To further investigate, we performed immunohistochemical analysis to determine whether Sagb expression levels were reduced in morphants. We found that the intensity of the immunostaining signal with the anti-Sag antibody in the whole pineal organ tended to decrease in morphant compared to control fish, although signals remained (Figures S2A–S2C), which was likely due to the expression of not only Sagb but also Saga, or to the poor knockdown effect of Sagb MOs. To find the knockdown effects in PP1 cells, we comparatively analyzed the signal intensity with anti-Sag antibody within anti-PP1 signals (Figures S2D and S2F) and found that the Sag signal clearly reduced in morphant compared to control fish (Figure S2G), suggesting knockdown effects with Sagb MOs in PP1 cells.

To verify any residual contribution of Sagb to PP1 photoresponses, we analyzed response profiles using Sagb and Arr3a double-knockdown fish. In the double-knockdown fish, we observed a profile with a gentler slope after the response peak compared with that of the Arr3a single-knockdown fish (Figure 3A, magenta open circle). Although statistical tests did not show a significant difference in amplitudes and slopes between Arr3a single- and double-knockdown fish (p = 0.7064 and 0.9909 in the comparisons of amplitudes and slopes, Tukey's multiple comparison test, Figure S3), we did find a significant difference in integrated areas (p = 0.0078, Tukey's multiple comparison test, Figure S3). Because the knockdown effects with Sagb MO1 were observed under the background of Arr3a knockdown, the contribution of Sagb was smaller than that of Arr3a but Sagb was potentially functional for PP1. Arr3a and Sagb may inactivate PP1 with different kinetics. To test this possibility of different kinetics between Arr3a and Sagb inactivation of PP1, we performed the imaging again using a stronger 405-nm light stimulus, which took more than

3 min for complete termination of the photoresponse in control fish (Figure 3B, gray closed circle). Interestingly, the stronger light flash led to observations opposite those obtained with a weaker light flash (Figure 3A). Briefly, Arr3a knockdown fish exhibited a similar response profile to control fish, whereas Sagb MO1 knockdown fish exhibited a dramatically different response profile (Figure 3B, skyblue oblique square and purple closed triangle, respectively). Note that knockdown fish with Sagb MO2 exhibited a similar profile to the Sagb MO1 one (Figure S2H). The slope of profile after the response peak in Sagb knockdown fish was clearly gentler than that in control and Arr3a knockdown fish (see the statistical analyses in Figure S3). Furthermore, the Sagb and Arr3a double-knockdown fish exhibited prolonged response compared with the Sagb single-knockdown fish, although the difference in slopes after the response peak between Sagb single- and double-knockdown fish was not significant (Figure 3B, magenta open circle; p = 0.972, Tukey's multiple comparison test, Figure S3). Accordingly, Arr3a may be potentially functional for the termination of photoresponse for a strong light flash but its contribution might be limited. Overall, these findings indicate that Arr3a is the major contributor to the response termination for weaker light flash, whereas Sagb is the major contributor to the response termination for stronger light flash. We found that PP1 inactivation by the two functional arrestins is switched in a light intensity–dependent manner in larval zebrafish PP1 cells (Figure 3F).

GRK-mediated function of Sagb and Arr3a in PP1 cells

Activated visual opsins such as rhodopsin and cone opsin by light stimulation are inactivated by arrestin binding following rhodopsin kinase-mediated phosphorylation.[2,10,30,31] In zebrafish PP1 cells, we previously reported that GRK7a is the major contributor to photoresponse termination processes among GRKs.[24] To understand how GRK7a cooperatively contributes to PP1 inactivation by switching Arr3a and Sagb in a light intensity-dependent manner, we investigated the photoresponse termination process using various gene knockdown fish by MOs containing those targeted GRKs. First, we evaluated whether Arr3a and Sagb inactivate PP1 in the presence of functional GRK7a using MOs of GRK7a, Arr3a, and Sagb. In the termination processes against both a weaker and stronger light flash, GRK7a single-knockdown fish and GRK7a/Arr3a double-knockdown fish exhibited similar profiles, indicating that Arr3a inactivated PP1 in a GRK7a-dependent manner (Figures 3C and 3D, green open square and light blue closed diamond). The profiles of response termination between GRK7a single- and GRK7a/Sagb double-knockdown fish were similar against a weaker light flash but not against a stronger light flash (Figures 3C and 3D, green open square and purple closed triangle). The slope in the response termination of GRK7a/Sagb double-knockdown fish against stronger light flash was clearly gentler than that of GRK7a single-knockdown fish, which was statistically supported ($p < 0.001$, Tukey's multiple comparison test, Figure S3). These observations raise two possibilities: Sagb functions either independently of phosphorylation or dependently on phosphorylation of PP1 by other residual GRKs for termination.

We then evaluated knockdown effects with GRK7b and/or GRK1b MOs under GRK7a knockdown background. The strongest effect on response terminations was observed in GRK7a/7b/1b triple-knockdown fish (Figure 3E, red closed triangle), followed by GRK7a/7b double-knockdown fish (Figure 3E, red open diamond). The residual contribution to the response termination processes observed in GRK7a/7b double-knockdown fish may be considered based on GRK1b. Similarly, a contribution to the response termination processes in GRK7a/1b double-knockdown fish is suggested based on GRK7b (Figure 3E, yellow closed diamond). We did not find large differences among GRK7a single-knockdown, GRK7b/1b double-knockdown, and control fish (Figure 3E, green open square, orange closed diamond, and gray closed circle). In contrast, GRK7a/7b/1b triple knockdown was highly effective on the response termination processes (Figure 3E, red closed triangle). Thus, the effects of GRK7a single knockdown and GRK7b/1b double knockdown are comparable. The lack of difference among partial knockdowns of GRKs indicates the complementary contributions of those to the termination process. These observations suggest that GRK7b and also presumably GRK1b contribute to the response termination processes in addition to GRK7a in control fish. In addition, the Sagb/GRK7a/GRK7b/GRK1b quadruple-knockdown effect was almost the same as the GRK7a/GRK7b/GRK1b triple-knockdown effect (Figure 3E, red open and closed triangles). Accordingly, we concluded that Sagb inactivates PP1 in the presence of functional GRKs, similar to Arr3a in PP1 cells.

A possible mechanism for the light intensity-dependent switching of the two arrestins based on their competitive binding to PP1

We found that Arr3a and Sagb function to inactivate PP1 under different intensities of light. In other words, inactivation by Arr3a is dominant when the amount of PP1 photoproduct is smaller, under a weaker light intensity; in contrast, inactivation by Sagb is dominant when the amount of photoproduct is larger, under a stronger light intensity. These observations raise the possibility that the two arrestins competitively bind to PP1 based on their own biding properties to PP1. We next investigated the binding of the two arrestins to PP1 using a split luciferase assay, a technique used to observe protein-protein interactions, such as those of G protein-coupled receptors (GPCRs) and arrestins, by using C-terminal and N-terminal split Emerald luciferase fragments (LucC and LucN, respectively, Figure 4A, left).[32] We observed an increase in luminescence upon 405-nm light irradiation in cultured cells co-expressing PP1-LucC with either LucN-Sagb or -Arr3a, indicating that the association between LucN and LucC was facilitated by the binding of Sagb or Arr3a to PP1 light-dependently (Figure 4B, blue open circle in top and bottom, respectively). These results demonstrate the binding of the two arrestins to the PP1 photoproduct in the cultured cells. To test a possibility of the competitive binding between the two arrestin to PP1, we additionally expressed the luciferase-free arrestin (Figure 4A, right, Luc-free Sagb or Luc-free Arr3a). We found that the luminescence increase resulting from the association of PP1-LucC and LucN-Sagb was significantly reduced when Luc-free Arr3a was co-expressed (Figure 4B green square

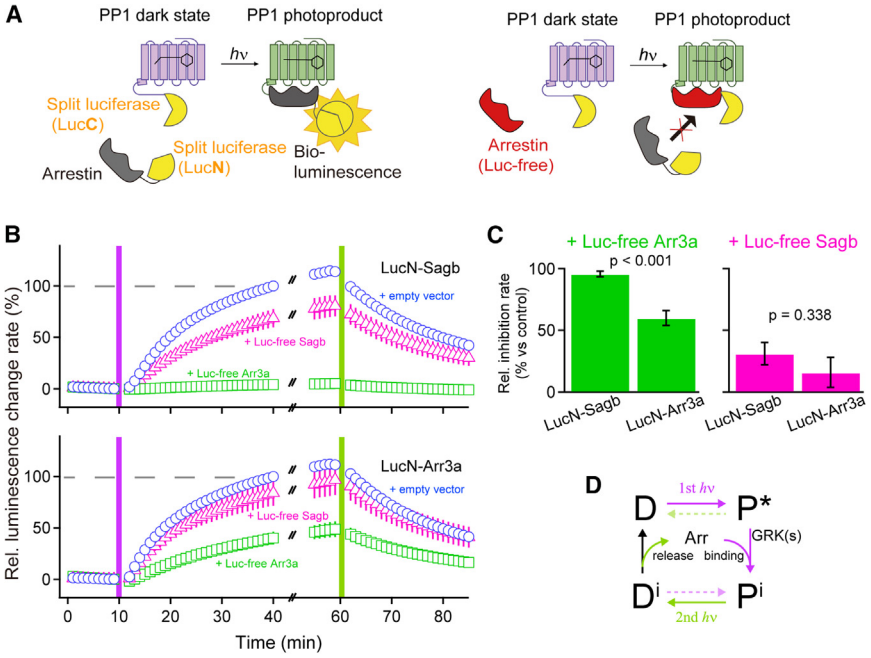

Figure 4. Investigations of affinity between arrestins and PP1 by split luciferase assay

(A) Schematic diagram of the split luciferase assay. The luciferase is separated into two parts (LucN and LucC). LucC is fused to PP1 C terminus (PP1-LucC) and LucN is fused to arrestins (LucN-Sagb and LucN-Arr3a). In addition to those components, by expressing luciferase-free arrestins (Luc-free Sagb and Luc-free Arr3a), competition can be observed according to affinity strength for PP1.

(B) The profiles of luminescence changes in response to light irradiation are averages obtained after standardizing by setting the luminescence change rate 30 min after UV irradiation in the control (+ empty vector, blue open circles) to 100% for each trial (n = 7). The magenta and green lines indicate light irradiation with 405-nm and 500-nm LED light, respectively. Note that the points after 40 min of recording time were adjusted according to the variance in the timing of the second light irradiation.

(C) Quantitative analyses of the relative inhibition rates of binding by expressing additional Luc-free arrestins (left, Luc-free Arr3a; right, Luc-free Sagb). p values were calculated by Welch's t test.

(D) A schematic presentation showing the reaction model in PP1-cells, where D, P*, P^i, and D^i indicate the PP1 dark state, active photoproduct, arrestin-bound photoproduct, and arrestin-bound dark state, respectively. Magenta and green arrows indicate major pathways accelerated after 405-nm (1st hν) and 500-nm (2 nd hν) LED light irradiation in B. The reaction pathways indicated by dotted arrows are theoretically accelerated by light irradiation, but the reaction cannot be judged from the profiles showing the association of LucN and LucC. Note: It is not known how the phosphorylated states of D and P are involved in the reaction model because they have not been investigated.

in top). We quantitatively and statistically evaluated the relative inhibition rates of binding by expressing Luc-free Arr3a with PP1-LucC and either LucN-Sagb or LucN-Arr3a, and found that Luc-free Arr3a significantly inhibited the binding between PP1-LucC and LucN-Sagb than between PP1-LucC and LucN-Arr3a (Figure 4C, left). In contrast, the relative inhibition rates of binding by additional expression of Luc-free Sagb were comparable (Figure 4B, magenta open triangle; Figure 4C, right). These observations demonstrate the Arr3a preferably binds to PP1 over Sagb in the competitive conditions, suggesting a possibility that Arr3a has a higher affinity than Sagb for PP1. The second stimulation with visible light caused a decrease in luminescence, indicating dissociations of LucN-arrestins and PP1-LucC by the back-reaction of the PP1 photoproduct to the dark state upon visible light absorption. From the viewpoint of PP1 bistability, these results suggest that the back-reaction induced by visible light facilitates the dissociation of arrestin and PP1 (see discussion).

DISCUSSION

In this study, we identified a rod-type arrestin, Sagb, and a cone-type arrestin, Arr3a, as arrestins inactivating the pineal opsin PP1. In the lamprey, parapinopsin couples to β-arrestin.[33] Melanopsin, a non-visual opsin in vertebrates, couples to two β-arrestins.[34] To our knowledge, this is the first report demonstrating that visual arrestins are involved in the inactivation of a non-visual opsin. We also found that cone- and rod-type GRKs (GRK7a/7b/1b) are involved in the inactivation of PP1. Together with our previous finding that a cone-type transducin Gt2 coupled to PP1,[21] we demonstrated that PP1 couples to various rod- and cone-type signal transduction-related proteins.

A possible physiological contribution of the switching of functional arrestins in the larval PP1 cells depending on light intensity

Here, we found a novel phenomenon of switching the contributions of two types of visual arrestins to the inactivation process depending on light intensity in the larval PP1 cells. Arr3a quickly inactivates PP1 photoproducts generated under weak light conditions, likely contributing to the formation of transient cell responses to UV in dim light environments. In contrast, Sagb inactivates a large number of PP1 photoproducts generated under strong light. The slower PP1 inactivation by Sagb than by Arr3a would be important in order for PP1 cells to detect "color information." The generation of color opponency requires the accumulation of abundant active PP1 photoproduct, indicating that, under strong light conditions, the slow inactivation involving Sagb is suitable to maintain the amount of active PP1 photoproduct. The arrestin-switching mechanism, corresponding to changes from dim to strong light, may contribute to the switch from irradiance to color detection in PP1 cells. Thus, the generation of PP1-based color opponency is expected to be limited to relatively strong light environments. This light intensity-dependent arrestin switching mechanism may be achieved with a sufficient amount of unbound Sagb remaining for PP1. We found that under weak light conditions in PP1 cells, Arr3a preferentially binds to PP1. In competitive binding experiments involving the two arrestins to PP1 in cultured cells, we observed that Arr3a competitively and significantly inhibits the binding of Sagb to

PP1. Thus, if the expression level of Sagb is higher than that of Arr3a, it can be speculated that Sagb becomes functional after the depletion of Arr3a to PP1 under strong light conditions. The different expression level between the rod and cone types of arrestins (ARR1 and ARR4, respectively) in cones has been reported in mouse. ARR1 is expressed 50-fold more abundantly than cone-type ARR4.[35] The expression profile of the two types of arrestins in mice is similar to the aforementioned speculation for Arr3a and Sagb in PP1 cells, although the mouse two arrestins, ARR1 and ARR4 are suggested to have play similar roles for cone cell photoresponses based on experimental results with each arrestin-knockout mice,[35] which is different from our findings, that is, light intensity-dependent functional switching between rod-type Sagb and cone-type Arr3a.

We may speculate mechanisms other than that described previously for the switching mechanism. In the case that the switching mechanism does not depend on the differences in expression levels between Sagb and Arr3a, unlike previous speculation, the phosphorylation of PP1 by different subtypes of GRK may be involved as an example. PP1 has nine threonine and serine residues at the C terminus that are potential phosphorylation sites. Therefore, GRK7a, 7b, and possibly 1b are thought to terminate G protein activation by PP1 photoproducts through phosphorylation of these candidate sites in the PP1 C terminus. Although the relationship between PP1 phosphorylation sites and the subtypes of GRK remains largely unclear, it is interesting to speculate a possibility that the order of the light intensity-dependent functioning of GRK subtypes, each of which could phosphorylate different amino acid residues at the C terminus to promote binding of different types of arrestin, enable the arrestin switching. Alternatively, it is also possible that subtypes of recoverin (S-modulin),[36–39] known as a regulator of GRK, inhibit specific GRK subtypes in a calcium-dependent manner. If such a mechanism involving different subtypes of GRK and/or recoverin exists, the difference in expression levels of the two arrestins described previously may not be important for the switching mechanism. Therefore, the relationship among PP1 phosphorylation, calcium dynamics, and the arrestin switching mechanism is an interesting issue in our future study.

We observed Arr3a expression in larval PP1 cells using immunohistochemistry (Figure 1I). However, Arr3a expression was not detected in adult PP1 cells by *in situ* hybridization (Figure 1G). The differences in Arr3a expression patterns between larval and adult stages may suggest age-dependent variations in the roles of PP1 cells, which is potentially interesting in the viewpoint of relationship with the arrestin switching mechanism in PP1 cells. However, considering that the comparative Arr3a-positive and -negative data were obtained from larval and adult zebrafish PP1 cells at single time points, respectively, using different methods, more detailed analyses, such as time course studies, will be necessary for detailed discussion.

Light inactivation versus dark inactivation in PP1 cells

We found that response profiles against weak light almost completely depend on the presence of GRK7a (Figure 3C). However, the PP1 photoresponses in the Sagb and Arr3a double-knockdown fish exhibited an extremely prolonged response against a strong light flash and termination was not observed (Figure 3B, magenta open circle), despite the presence of GRKs. These observations may be explained by slight G protein activation by phosphorylated PP1 photoproducts, together with a shortage of arrestins, according to previous reports; in the rod arrestin KO mouse, clear prolongation of the response is observed,[10] suggesting that phosphorylated photoproducts without the arrestin activate G protein at a lower level. We can speculate that, under the relatively strong light conditions in which PP1 cells generate color opponency, the amount of arrestin in PP1 cells is insufficient to bind all of the light-activated PP1 and completely inactivate the G protein activation, suggesting that phosphorylated "stable PP1 photoproduct" could sustainably activate G protein to generate a prolonged response. We found that visible light causes dissociation of the binding between arrestins and PP1 (Figure 4B). A simplified reaction model involving UV and visible light photoreaction of PP1, without considering phosphorylated states, is shown in Figure 4D. The observations in visible light irradiation suggest that the back-reaction from the arrestin-bound photoproduct to the arrestin-bound dark state led to dissociation of the PP1-arrestin complex (Figure 4D, solid green arrows). In this context, we can speculate that the release of arrestin from PP1 by visible light helps sustainably supply an adequate amount of arrestin available for inactivating the active PP1 photoproduct to maintain a constant G protein activation level, even in photoequilibrium under relatively strong light conditions where PP1 cells can generate color information.

Limitations of the study

This study highlights the significance of multiple arrestin expressions within a cell. Knockdown by microinjection of morpholino antisense oligos into zebrafish embryos proved highly useful for investigating larval systems involving cooperative functions of multiple genes, as demonstrated in our research. However, we observed potential differences in arrestin expression between larval and adult zebrafish. Investigation of these differences was precluded in this study due to the technical challenges of performing knockdowns in adult fish using morpholino antisense oligos. Future research focusing on adult zebrafish would benefit from employing knockout lines. While generating knockout fish using CRISPR-Cas9-mediated genome editing is a promising alternative to morpholinos, targeting multiple genes would require a complex and time-consuming process to obtain results and conclusions. To obtain the findings presented in this paper using adult zebrafish instead of the larvae would require extensive and repeated crossings of knockout lines, making studies in adult fish a long-term endeavor.

RESOURCE AVAILABILITY

Lead contact

Further information and requests for resources and reagents should be directed to and will be fulfilled by the lead contact, Akihisa Terakita (terakita@omu.ac.jp).

Materials availability

This study did not generate new unique reagents.

Data and code availability

- All data that support the findings of this study are available from the lead contact upon reasonable request.
- This study does not generate any original code.
- Any additional information required to reanalyze the data reported in this paper is available from the lead contact upon reasonable request.

ACKNOWLEDGMENTS

This work was supported by Japan Society for the Promotion of Sciences Grants-in-Aid for Scientific Research (JSPS KAKENHI) JP15H05777 and JP23H02516 (to A.T.), JP18H02482 and JP22H02663 (to M.K.), JP21K06265 (to E.K.-Y.), JP18K14751 and JP20K15844 (to S.W.), JP22H00322 (to T.O.) and Japan Science and Technology Agency Core Research for Evolutional Science and Technology (JST CREST) JPMJCR1753 (to A.T.).

AUTHOR CONTRIBUTIONS

All authors had full access to all the data in the study and take responsibility for the integrity of the data and accuracy of the data analysis. B.S., S.W., M.K., and A.T. designed the research. B.S. and H.N. performed experiments. S.W., T.S., E.K.-Y., T.N., and T.O. aided in the development of experimental techniques. B.S., S.W., M.K., and A.T. wrote the manuscript. All authors read and approved the final manuscript.

DECLARATION OF INTERESTS

The authors declare no competing interests.

STAR★METHODS

Detailed methods are provided in the online version of this paper and include the following:

- KEY RESOURCES TABLE
- EXPERIMENTAL MODEL AND STUDY PARTICIPANT DETAILS
  - Cell line
  - Animals
- METHOD DETAILS
  - *In situ* hybridization
  - Whole-mount immunohistochemistry
  - Antisense morpholino oligonucleotide-mediated knockdown
  - Two-photon imaging
  - Split luciferase assay
- QUANTIFICATION AND STATISTICAL ANALYSIS

SUPPLEMENTAL INFORMATION

Supplemental information can be found online at https://doi.org/10.1016/j.isci.2024.111706.

Received: July 16, 2024
Revised: October 22, 2024
Accepted: December 26, 2024
Published: December 28, 2024

REFERENCES

1. Chen, J., Makino, C.L., Peachey, N.S., Baylor, D.A., and Simon, M.I. (1995). Mechanisms of rhodopsin inactivation in vivo as revealed by a COOH-terminal truncation mutant. Science *267*, 374–377. https://doi.org/10.1126/science.7824934.
2. Hurley, J.B., Spencer, M., and Niemi, G.A. (1998). Rhodopsin phosphorylation and its role in photoreceptor function. Vision Res. *38*, 1341–1352. https://doi.org/10.1016/s0042-6989(97)00459-8.
3. Kuhn, H. (1978). Light-regulated binding of rhodopsin kinase and other proteins to cattle photoreceptor membranes. Biochemistry *17*, 4389–4395. https://doi.org/10.1021/bi00614a006.
4. Kuhn, H., Hall, S.W., and Wilden, U. (1984). Light-induced binding of 48-kDa protein to photoreceptor membranes is highly enhanced by phosphorylation of rhodopsin. FEBS Lett. *176*, 473–478. https://doi.org/10.1016/0014-5793(84)81221-1.
5. Lyubarsky, A.L., Chen, C., Simon, M.I., and Pugh, E.N. (2000). Mice lacking G-protein receptor kinase 1 have profoundly slowed recovery of cone-driven retinal responses. J. Neurosci. *20*, 2209–2217.
6. Maeda, T., Imanishi, Y., and Palczewski, K. (2003). Rhodopsin phosphorylation: 30 years later. Prog. Retin. Eye Res. *22*, 417–434. https://doi.org/10.1016/s1350-9462(03)00017-x.
7. Ohguro, H., Van Hooser, J.P., Milam, A.H., and Palczewski, K. (1995). Rhodopsin phosphorylation and dephosphorylation in vivo. J. Biol. Chem. *270*, 14259–14262. https://doi.org/10.1074/jbc.270.24.14259.
8. Tachibanaki, S., Arinobu, D., Shimauchi-Matsukawa, Y., Tsushima, S., and Kawamura, S. (2005). Highly effective phosphorylation by G protein-coupled receptor kinase 7 of light-activated visual pigment in cones. Proc. Natl. Acad. Sci. USA *102*, 9329–9334. https://doi.org/10.1073/pnas.0501875102.
9. Wilden, U., Hall, S.W., and Kühn, H. (1986). Phosphodiesterase activation by photoexcited rhodopsin is quenched when rhodopsin is phosphorylated and binds the intrinsic 48-kDa protein of rod outer segments. Proc. Natl. Acad. Sci. USA *83*, 1174–1178. https://doi.org/10.1073/pnas.83.5.1174.
10. Xu, J., Dodd, R.L., Makino, C.L., Simon, M.I., Baylor, D.A., and Chen, J. (1997). Prolonged photoresponses in transgenic mouse rods lacking arrestin. Nature *389*, 505–509. https://doi.org/10.1038/39068.
11. Zhu, X., Brown, B., Li, A., Mears, A.J., Swaroop, A., and Craft, C.M. (2003). GRK1-dependent phosphorylation of S and M opsins and their binding to cone arrestin during cone phototransduction in the mouse retina. J. Neurosci. *23*, 6152–6160.
12. Caenepeel, S., Charydczak, G., Sudarsanam, S., Hunter, T., and Manning, G. (2004). The mouse kinome: discovery and comparative genomics of all mouse protein kinases. Proc. Natl. Acad. Sci. USA *101*, 11707–11712. https://doi.org/10.1073/pnas.0306880101.
13. Weiss, E.R., Ducceschi, M.H., Horner, T.J., Li, A., Craft, C.M., and Osawa, S. (2001). Species-specific differences in expression of G-protein-coupled receptor kinase (GRK) 7 and GRK1 in mammalian cone photoreceptor cells: implications for cone cell phototransduction. J. Neurosci. *21*, 9175–9184. https://doi.org/10.1523/JNEUROSCI.21-23-09175.2001.
14. Wada, Y., Sugiyama, J., Okano, T., and Fukada, Y. (2006). GRK1 and GRK7: unique cellular distribution and widely different activities of opsin phosphorylation in the zebrafish rods and cones. J. Neurochem. *98*, 824–837. https://doi.org/10.1111/j.1471-4159.2006.03920.x.
15. Craft, C.M., and Deming, J.D. (2014). Cone Arrestin: Deciphering the Structure and Functions of Arrestin 4 in Vision. In Arrestins - Pharmacology and Therapeutic Potential, V.V. Gurevich, ed. (Springer Berlin Heidelberg), pp. 117–131. https://doi.org/10.1007/978-3-642-41199-1_6.
16. Renninger, S.L., Gesemann, M., and Neuhauss, S.C.F. (2011). Cone arrestin confers cone vision of high temporal resolution in zebrafish larvae. Eur. J. Neurosci. *33*, 658–667. https://doi.org/10.1111/j.1460-9568.2010.07574.x.
17. Dodt, E. (1962). [Comparative studies on the adaptive behavior of the pure cone retina. Citellus citellus, Sciurus vulgaris]. Pflugers Arch. für Gesamte Physiol. Menschen Tiere *275*, 561–573.
18. Dodt, E. (1973). The parietal eye (pineal and parietal organs) of lower vertebrates. In Visual Centers in the Brain, R. Jung, ed. (Springer Berlin Heidelberg), pp. 113–140. https://doi.org/10.1007/978-3-642-65495-4_4.
19. Dodt, E., and Heerd, E. (1962). Mode of action of pineal nerve fibers in frogs. J. Neurophysiol. *25*, 405–429. https://doi.org/10.1152/jn.1962.25.3.405.

20. Falcon, J., Marmillon, J.B., Claustrat, B., and Collin, J.P. (1989). Regulation of melatonin secretion in a photoreceptive pineal organ: an in vitro study in the pike. J. Neurosci. *9*, 1943–1950.

21. Koyanagi, M., Wada, S., Kawano-Yamashita, E., Hara, Y., Kuraku, S., Kosaka, S., Kawakami, K., Tamotsu, S., Tsukamoto, H., Shichida, Y., and Terakita, A. (2015). Diversification of non-visual photopigment parapinopsin in spectral sensitivity for diverse pineal functions. BMC Biol. *13*, 73. https://doi.org/10.1186/s12915-015-0174-9.

22. Blackshaw, S., and Snyder, S.H. (1997). Parapinopsin, a novel catfish opsin localized to the parapineal organ, defines a new gene family. J. Neurosci. *17*, 8083–8092. https://doi.org/10.1523/JNEUROSCI.17-21-08083.1997.

23. Koyanagi, M., Kawano, E., Kinugawa, Y., Oishi, T., Shichida, Y., Tamotsu, S., and Terakita, A. (2004). Bistable UV pigment in the lamprey pineal. Proc. Natl. Acad. Sci. USA *101*, 6687–6691. https://doi.org/10.1073/pnas.0400819101.

24. Shen, B., Wada, S., Nishioka, H., Nagata, T., Kawano-Yamashita, E., Koyanagi, M., and Terakita, A. (2021). Functional identification of an opsin kinase underlying inactivation of the pineal bistable opsin parapinopsin in zebrafish. Zoological Lett. *7*, 1. https://doi.org/10.1186/s40851-021-00171-1.

25. Wada, S., Kawano-Yamashita, E., Koyanagi, M., and Terakita, A. (2012). Expression of UV-sensitive parapinopsin in the iguana parietal eyes and its implication in UV-sensitivity in vertebrate pineal-related organs. PLoS One *7*, e39003. https://doi.org/10.1371/journal.pone.0039003.

26. Wada, S., Shen, B., Kawano-Yamashita, E., Nagata, T., Hibi, M., Tamotsu, S., Koyanagi, M., and Terakita, A. (2018). Color opponency with a single kind of bistable opsin in the zebrafish pineal organ. Proc. Natl. Acad. Sci. USA *115*, 11310–11315. https://doi.org/10.1073/pnas.1802592115.

27. Terakita, A., Koyanagi, M., Tsukamoto, H., Yamashita, T., Miyata, T., and Shichida, Y. (2004). Counterion displacement in the molecular evolution of the rhodopsin family. Nat. Struct. Mol. Biol. *11*, 284–289. https://doi.org/10.1038/nsmb731.

28. Wilbanks, A.M., Fralish, G.B., Kirby, M.L., Barak, L.S., Li, Y.-X., and Caron, M.G. (2004). ß-Arrestin 2 Regulates Zebrafish Development Through the Hedgehog Signaling Pathway. Science *306*, 2264–2267. https://doi.org/10.1126/science.1104193.

29. Yue, R., Kang, J., Zhao, C., Hu, W., Tang, Y., Liu, X., and Pei, G. (2009). Arrestin1 Regulates Zebrafish Hematopoiesis through Binding to YY1 and Relieving Polycomb Group Repression. Cell *139*, 535–546. https://doi.org/10.1016/j.cell.2009.08.038.

30. Baylor, D.A., and Burns, M.E. (1998). Control of rhodopsin activity in vision. Eye *12*, 521–525. https://doi.org/10.1038/eye.1998.140.

31. Berry, J., Frederiksen, R., Yao, Y., Nymark, S., Chen, J., and Cornwall, C. (2016). Effect of Rhodopsin Phosphorylation on Dark Adaptation in Mouse Rods. J. Neurosci. *36*, 6973–6987. https://doi.org/10.1523/jneurosci.3544-15.2016.

32. Hida, N., Awais, M., Takeuchi, M., Ueno, N., Tashiro, M., Takagi, C., Singh, T., Hayashi, M., Ohmiya, Y., and Ozawa, T. (2009). High-sensitivity real-time imaging of dual protein-protein interactions in living subjects using multicolor luciferases. PLoS One *4*, e5868. https://doi.org/10.1371/journal.pone.0005868.

33. Kawano-Yamashita, E., Koyanagi, M., Shichida, Y., Oishi, T., Tamotsu, S., and Terakita, A. (2011). beta-arrestin functionally regulates the non-bleaching pigment parapinopsin in lamprey pineal. PLoS One *6*, e16402. https://doi.org/10.1371/journal.pone.0016402.

34. Cameron, E.G., and Robinson, P.R. (2014). beta-Arrestin-dependent deactivation of mouse melanopsin. PLoS One *9*, e113138. https://doi.org/10.1371/journal.pone.0113138.

35. Nikonov, S.S., Brown, B.M., Davis, J.A., Zuniga, F.I., Bragin, A., Pugh, E.N., Jr., and Craft, C.M. (2008). Mouse Cones Require an Arrestin for Normal Inactivation of Phototransduction. Neuron *59*, 462–474. https://doi.org/10.1016/j.neuron.2008.06.011.

36. Kawamura, S. (1993). Rhodopsin phosphorylation as a mechanism of cyclic GMP phosphodiesterase regulation by S-modulin. Nature *362*, 855–857. https://doi.org/10.1038/362855a0.

37. Gorodovikova, E.N., Senin, I.I., and Philippov, P.P. (1994). Calcium-sensitive control of rhodopsin phosphorylation in the reconstituted system consisting of photoreceptor membranes, rhodopsin kinase and recoverin. FEBS Lett. *353*, 171–172. https://doi.org/10.1016/0014-5793(94)01030-7.

38. Klenchin, V.A., Calvert, P.D., and Bownds, M.D. (1995). Inhibition of rhodopsin kinase by recoverin. Further evidence for a negative feedback system in phototransduction. J. Biol. Chem. *270*, 16147–16152. https://doi.org/10.1074/jbc.270.27.16147.

39. Zang, J., Keim, J., Kastenhuber, E., Gesemann, M., and Neuhauss, S.C.F. (2015). Recoverin depletion accelerates cone photoresponse recovery. Open Biol. *5*, 150086. https://doi.org/10.1098/rsob.150086.

40. Schindelin, J., Arganda-Carreras, I., Frise, E., Kaynig, V., Longair, M., Pietzsch, T., Preibisch, S., Rueden, C., Saalfeld, S., Schmid, B., et al. (2012). Fiji: an open-source platform for biological-image analysis. Nat. Methods *9*, 676–682. https://doi.org/10.1038/nmeth.2019.

41. Sun, L., Kawano-Yamashita, E., Nagata, T., Tsukamoto, H., Furutani, Y., Koyanagi, M., and Terakita, A. (2014). Distribution of mammalian-like melanopsin in cyclostome retinas exhibiting a different extent of visual functions. PLoS One *9*, e108209. https://doi.org/10.1371/journal.pone.0108209.

42. Randlett, O., Wee, C.L., Naumann, E.A., Nnaemeka, O., Schoppik, D., Fitzgerald, J.E., Portugues, R., Lacoste, A.M.B., Riegler, C., Engert, F., and Schier, A.F. (2015). Whole-brain activity mapping onto a zebrafish brain atlas. Nat. Methods *12*, 1039–1046. https://doi.org/10.1038/nmeth.3581.

STAR★METHODS

KEY RESOURCES TABLE

REAGENT or RESOURCE	SOURCE	IDENTIFIER
Antibodies		
Anti-PP1 antibody	Koyanagi et al.[21]	N/A
Anti-Sag antibody	EnCor Biotechnology Inc.	Cat# MCA-S128; RRID: AB_2572227
zpr-1 (Anti-Arr3a antibody)	ZIRC	ZFIN: ZDB-ATB-081002-43 RRID: AB_10013803
Chemicals, peptides, and recombinant proteins		
Tricane	Sigma-Aldrich	MS-222
Experimental models: Organisms/strains		
Zebrafish: Tg(pp1: GCaMP6s)	Wada et al.[26]	ZFIN ID: ZDB-ALT-220321-3
Oligonucleotides		
Morpholino: Sagb MO1 5′-AATCTCGCTTCCCCATGTAAACGCC-3′	Gene Tools	N/A
Morpholino: Sagb MO2 5′-TGTGCTTGGGACTCATTCTGTCTCC-3′	Gene Tools	N/A
Morpholino: GRK7a MO1 5′-ATCGAGTCCCCCCATGTCACACATT-3′	Gene Tools	ZFIN: ZDB-MRPHLNO-050824-1
Morpholino: GRK7b MO1 5′-CTTCAGTCCACCCATGTCACTCATG-3′	Gene Tools	ZFIN: ZDB-MRPHLNO-211015-4
Morpholino: GRK1b MO1 5′-AGTCTCCAAACCTCCAATATCCATG-3′	Gene Tools	ZFIN: ZDB-MRPHLNO-211015-1
Morpholino: Arr3a MO1 5′-ATAATCCGCAGCCCGTCTGGTGTAG-3′	Gene Tools	ZFIN: ZDB-MRPHLNO-110303-1
Morpholino: Arr3a MO2 5′-TTTCCTGTTCACTGGTAGAGCGATG-3′	Gene Tools	N/A
Morpholino: standard control MO 5′-CCTCTTACCTCATTACAATTTATA-3′	Gene Tools	N/A
Software and algorithms		
ImageJ/Fiji	Schindelin et al.[40]	https://fiji.sc/
Python3.10.15	Anaconda 3	https://www.anaconda.com/
Other		
Two-photon microscope	Olympus	FVMPE-RS

EXPERIMENTAL MODEL AND STUDY PARTICIPANT DETAILS

Cell line

HEK293S cell line was maintained in Dulbecco's Modified Eagle Medium (DMEM) + Glutamax (Gibco) supplemented with 10% FBS (Gibco) and 10 IU/mL penicillin–streptomycin at 37°C and 5% CO_2. The culture medium was replaced every two days during passage. The cell line was authenticated and confirmed to be free of mycoplasma contamination.

Animals

Zebrafish were maintained on 14-h light/10-h dark cycles at 28.5°C. Embryos were maintained in E3 medium (5 mM NaCl, 0.17 mM KCl, 0.33 mM $CaCl_2$, and 0.33 mM $MgSO_4$). The animal experiment procedures were approved by the Osaka City University Animal Experiment Committee (no. S0032) and complied with the regulations on animal experiments from Osaka City University.

METHOD DETAILS

In situ hybridization

The preparation of RNA probes and *in situ* hybridization were performed as previously described.[41] Digoxigenin (DIG)- and fluorescein-labeled antisense and sense RNA probes for zebrafish PP1, Saga, Sagb, Arr3a, Arr3b, β-arr1, β-arr2a, and β-arr2b were

synthesized using the DIG RNA labeling kit or fluorescein RNA labeling kit (Roche). The length of each RNA probes was as follows: zebrafish PP1 (full-length coding sequence, accession number, AB626966), Saga (full-length coding sequence, accession number, BC056570), Sagb (full-length coding sequence, accession number, BC080258), Arr3a (1 to 1249 bases of coding sequence, accession number, AY900006), Arr3b (20 to 1070 bases of coding sequence, accession number, BC152655), β-arr1 (full-length coding sequence, accession number, DQ508020), β-arr2a (full-length coding sequence, accession number, BC165790), and β-arr2b (full-length coding sequence, accession number, BC164508). Sections were pretreated with proteinase K and hybridized with each RNA probe in ULTRAhyb Ultrasensitive Hybridization Buffer (Ambion). For single staining, the probe was detected using the alkaline phosphatase-conjugated anti-digoxigenin antibody (Roche), followed by a blue 5-bromo-4-chloro-3-indolyl phosphate nitro blue tetrazolium color reaction. For double staining, the fluorescence labelling using the HNPP Fluorescent Detection Set (Roche) and an Alexa 488-conjugated anti-DNP antibody mediated with the TSA plus DNP (HRP) system (Perkin Elmer) was performed. Fluorescence images were acquired using a confocal microscope (Leica TCS SP8).

Whole-mount immunohistochemistry

Whole-mount immunohistochemistry was performed as previously described,[42] with slight modifications. In brief, larvae (5 days post-fertilization [dpf]) were fixed with 4% paraformaldehyde overnight at 4°C, washed with PBS-Tween (PBST), and treated with 150 mM Tris-HCl (pH 9.0) for 15 min at 70°C. Subsequently, the larvae were washed with PBST, treated with 0.05% Trypsin-EDTA for 45 min on ice, washed in PBST, and blocked in PBST containing 1% bovine serum albumin (BSA), 2% normal goat serum, and 1% dimethyl sulfoxide (blocking buffer). The larvae were incubated in 1:500 primary antibodies, anti-PP1,[21] anti-Sag (#MCA-S128, EnCor Biotechnology Inc.), and anti-Arr3a (zpr-1 from Zebrafish International Resource Center) antibodies in blocking buffer at 4°C overnight. The larvae were washed with PBST followed by incubation with 1:500 secondary antibodies (Alexa 594- and Alexa 647-conjugated goat anti-rabbit and anti-mouse IgG antibodies, Thermo Fisher Scientific) in PBST containing 1% BSA and 1% dimethyl sulfoxide (DMSO). Fluorescence images were acquired using a confocal microscope (Leica TCS SP8). The quantification of fluorescence intensity in the images was performed using ImageJ/Fiji.[40]

Antisense morpholino oligonucleotide-mediated knockdown

Sequences of antisense morpholino oligonucleotides (MOs) for zebrafish Sagb and GRK7a, and standard control were as follows: Sagb MO1, 5′-AATCTCGCTTCCCCATGTAAACGCC-3′; Sagb MO2, 5′-TGTGCTTGGGACTCATTCTGTCTCC-3′; GRK7a MO1, 5′-ATCGAGTCCCCCCATGTCACACATT-3′[24]; GRK7b MO1, 5′-CTTCAGTCCACCCATGTCACTCATG-3′[24]; GRK1b MO1, 5′-AGTC TCCAAACCTCCAATATCCATG-3′[24]; Arr3a MO1, 5′-ATAATCCGCAGCCCGTCTGGTGTAG-3′[16]; Arr3a MO2, 5′-TTTCCTGTTCA CTGGTAGAGCGATG-3′; standard control MO, 5′-CCTCTTACCTCATTACAATTTATA-3′. Each MO (0.2 mM, ∼2 nL) was injected into the yolk, close to the animal pole, at the 1-cell stage obtained from two strains, wild type and *Tg(pp1:GCaMP6s)*.

Two-photon imaging

Two-photon imaging was performed as previously described.[24] In brief, 5 dpf larvae were mounted dorsal side up in low-melting agarose gel (1.5% in E3 medium) on 35-mm glass-bottomed dishes (Iwaki). To prevent drying and to immobilize the larvae, E3 medium containing 0.002% tricaine (MS222, Sigma) was added to the dishes. Two-photon imaging was performed using an FVMPE-RS instrument (Olympus). Fluorescence intensities were calculated using ImageJ (https://imagej.net/ij/). Net fluorescence intensity was calculated by subtraction of mean fluorescence intensity between each region of interest containing PP1 cells and the nonfluorescent region outside PP1 cells (background). To prevent activation of opsins by two-photon excitation, two-image acquisitions, performed before and after the 405-nm laser flash, were repeated. The time intervals were modified corresponding to the stimulation of 405-nm light intensity. Under weak and strong light conditions, 14 (0.5, 1, 2, 3, 5, 7, 9, 10, 15, 20, 25, 30, 35, and 40 s) and 11 (0.5, 5, 10, 20, 40, 60, 80, 100, 120, 140, and 160 s) time intervals were set from the 405-nm laser flash to image acquisition, respectively. The series of ΔF/F values in each interval was calculated and plotted for time axis and shown as the profile of calcium response. Each 405-nm laser intensity used for stimulation under "weak" (Figures 2E, 2F, 3A, and 3C) and "strong" (Figures 3B, 3D, and 3E) light conditions was $\sim 4.3 \times 10^{14}$ and $\sim 5.0 \times 10^{16}$ photons/cm^2/s, respectively. Light intensity was calculated based on the size of the scanning area ($\sim$0.0064 mm^2).

Split luciferase assay

Interactions between PP1 and the two arrestins, Arr3a and Sagb, were observed using a split luciferase assay.[32] The cDNA sequence coding PP1 followed by C-terminal Eluc (PP1-LucC) and the cDNA sequences coding Arr3a and Sagb following the sequence coding N-terminal Eluc were constructed (LucN-Arr3a and LucN-Sagb, respectively) into the pcDNA3.1 expression vector. HEK293S cells (20%-30% confluent) in 35-mm tissue culture dishes were transfected with PP1-LucC (1.5 μg) and LucN-Arr3a or LucN-Sagb (0.3 μg) using the polyethyleneimine (PEI) transfection method. To observe the competition between Arr3a and Sagb, LucN-free Sagb, Arr3a and empty vector (0.3 μg) were simultaneously transfected. At ∼2 hours after transfection, 11-*cis* retinal (200 nM) was supplied to the medium followed by overnight incubation. Before the luminescence change recording, mediums were replaced with a CO_2-independent medium containing 10% FBS and GloSensor cAMP Reagent stock solution (Promega). Luminescence, representing the luciferase-association with interaction between PP1 and arrestins, was measured at 25°C using a GloMax 20/20n Luminometer

(Promega). The relative inhibition rate of binding by the additional expression of Luc-free arrestins was calculated in each trial (n = 7), using the luminescence change rate 30 minutes after UV irradiation in the control (+empty vector in Figure 4B) as 100%.

QUANTIFICATION AND STATISTICAL ANALYSIS

Pineal size (Figure 2C) and GCaMP6s fluorescence intensity (Figure 2D) in PP1 cells were quantified using ImageJ/Fiji software. Statistical analyses for these data were conducted with Dunnett's tests in Python 3. Sample sizes (n, the number of individuals) are indicated in the graphs, along with the mean and standard deviation. Statements of statistical significance are described in the figure legends. The statistical evaluations of calcium change profiles presented in Figures 2E and 2F, and 3A–3E are summarized in Figure S3, where Tukey's multiple comparison tests were performed using Python 3, along with the mean and 95% confidence intervals. Note that sample sizes (n, the number of individuals) are provided in graphs and the legends of Figures 2 and 3. Relative inhibition rate of luminescence intensity changes were shown with the mean and standard error of the mean (Figure 4C), which were calculated in Microsoft Excel. Welch's t tests were also performed in Microsoft Excel. P values are listed in the graphs. Sample sizes (n, the number of trials) are described in the legends. All data collection and analyses were conducted in a blinded fashion.